Advances in Mathematics 301 (2016) 711–738

Contents lists available at ScienceDirect

Advances in Mathematics

www.elsevier.com/locate/aim

A bifurcation phenomenon of Stokes curves around a double turning point, and influence of virtual turning points upon the transition probabilities for three-level systems

Shinji Sasaki

Research Institute for Mathematical Sciences, Kyoto University, Kyoto, 606-8502 Japan

ARTICLE INFO

Article history:
Received 28 October 2015
Received in revised form 22 June 2016
Accepted 29 June 2016
Available online 7 July 2016
Communicated by Takahiro Kawai

MSC:
34M40
34M60
34M25

Keywords:
Non-adiabatic transition
Three-level system
Exact WKB analysis
Virtual turning point
New Stokes curve

ABSTRACT

We study the non-adiabatic transition problem of three-level systems from the viewpoint of the exact WKB analysis. We show the importance of virtual turning points and new Stokes curves in this problem by presenting some concrete examples where the contribution of virtual turning points to transition probabilities becomes greater than that of ordinary turning points. In the course of our discussion we encounter a bifurcation phenomenon of Stokes curves around a double turning point, and we investigate this issue as well.

E-mail address: sasaki@kurims.kyoto-u.ac.jp.

http://dx.doi.org/10.1016/j.aim.2016.06.025
0001-8708/

1. Introduction

We study the non-adiabatic transition problem of three-level systems from the viewpoint of the exact WKB analysis and discuss the importance of new Stokes curves and virtual turning points in this problem.

There have been many works on non-adiabatic transition problems of three-level systems (cf. [6,5,11] and references cited there). Exact WKB theoretic study of this problem is done in [3] and the role of virtual turning points and new Stokes curves in this problem is discussed in [16,14]. Necessity of new Stokes curves for systems of differential equations (or higher order single equations) was first recognized by Berk, Nevins and Roberts [4], and later Aoki, Kawai and Takei [2] introduced the notion of virtual turning points to interpret new Stokes curves as Stokes curves emanating from virtual turning points. We refer the reader to [10] for the definition of virtual turning points, related notions and their basic properties. In this paper we present some concrete examples where the contribution of virtual turning points to the transition probabilities is greater than that of ordinary turning points and discuss a bifurcation phenomenon of Stokes curves around a double turning point which is closely related to this problem.

Following [3], we consider the equation

$$i\frac{d}{dt}\Psi = \eta H(t,\eta)\Psi, \tag{1}$$

where $\Psi = \Psi(t,\eta)$ is a 3-vector, $\eta > 0$ is a large parameter and $H(t,\eta)$ is a 3×3 matrix given below:

$$\begin{aligned} H(t,\eta) &= H_0(t) + \eta^{-1/2}H_{1/2} \\ &= \begin{pmatrix} \rho_1(t) & 0 & 0 \\ 0 & \rho_2(t) & 0 \\ 0 & 0 & \rho_3(t) \end{pmatrix} + \eta^{-1/2}\begin{pmatrix} 0 & c_{12} & c_{13} \\ \overline{c_{12}} & 0 & c_{23} \\ \overline{c_{13}} & \overline{c_{23}} & 0 \end{pmatrix} \end{aligned} \tag{2}$$

with real polynomials $\rho_1(t)$, $\rho_2(t)$, $\rho_3(t)$ and complex constants c_{12}, c_{13}, c_{23}. This equation, especially continuation problem of solutions between $-\infty$ and $+\infty$, is studied in [3] from the viewpoint of the exact WKB analysis. The Stokes geometry, namely the configuration of the turning points (i.e., zeros of $\rho_j - \rho_k$ $(j,k = 1,2,3)$) and the Stokes curves (i.e., curves defined by $\mathrm{Im}[(1/i)\int_{t_0}^{t}(\rho_j(s)-\rho_k(s))\,ds] = 0$ ($j,k = 1,2,3$ and t_0 is a turning point)), is important there. In order to illustrate the Stokes geometry concretely with the aid of a computer, we consider the following example.

Example 1. $\rho_1(t) = t^2 + 1 + i\epsilon_1$, $\rho_2(t) = 0$ and $\rho_3(t) = t^2 + 4 + i\epsilon_2$.

Though we basically want ρ_j's to be real, the Stokes geometry is degenerate when $\epsilon_1 = \epsilon_2 = 0$ (Fig. 1). So we consider this example with ϵ_1 and ϵ_2 small but nonzero. If $\epsilon_1 = 0.02$ and $\epsilon_2 = 0.1$, the Stokes geometry is given by Fig. 2. Here virtual turning points

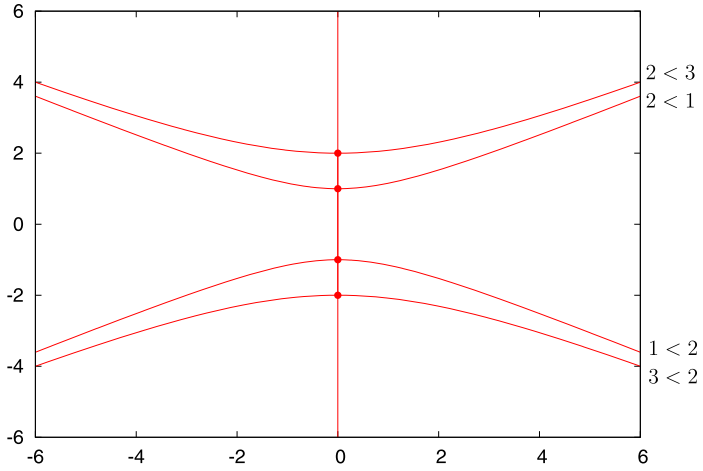

Fig. 1. Turning points and ordinary Stokes curves for Example 1 with $\epsilon_1 = \epsilon_2 = 0$.

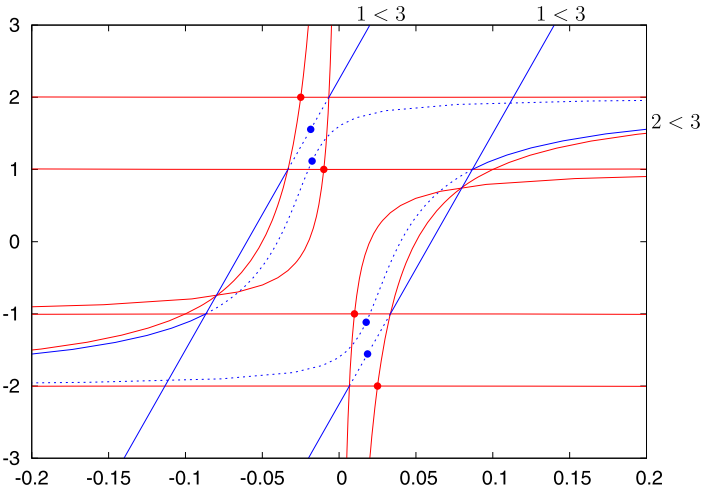

Fig. 2. Stokes geometry for Example 1 with $\epsilon_1 = 0.02$ and $\epsilon_2 = 0.1$. (For interpretation of the references to color in this figure legend, the reader is referred to the web version of this article.)

and new Stokes curves are included to complete the Stokes geometry. (Throughout this paper, ordinary turning points and ordinary Stokes curves are designated by red, and virtual turning points and new Stokes curves are by blue. Dotted lines represent inert (vs. active) portions of Stokes curves, i.e., portions of Stokes curves where the Stokes coefficients are zero. We remark that new Stokes curves are always inert near virtual turning points. See [10,3] for details.) Meanwhile if $\epsilon_1 = 0.09$ and $\epsilon_2 = 0.1$, the Stokes geometry is Fig. 3. This is rather different from Fig. 2. Especially the positions of the Stokes curves near the real axis are interchanged. Now letting ϵ_1 move from 0.02 to 0.09 with $\epsilon_2 = 0.1$ fixed, we follow how the Stokes geometry changes. The figures are given in Fig. 4. We focus on the Stokes curve which emanates downward from the turning

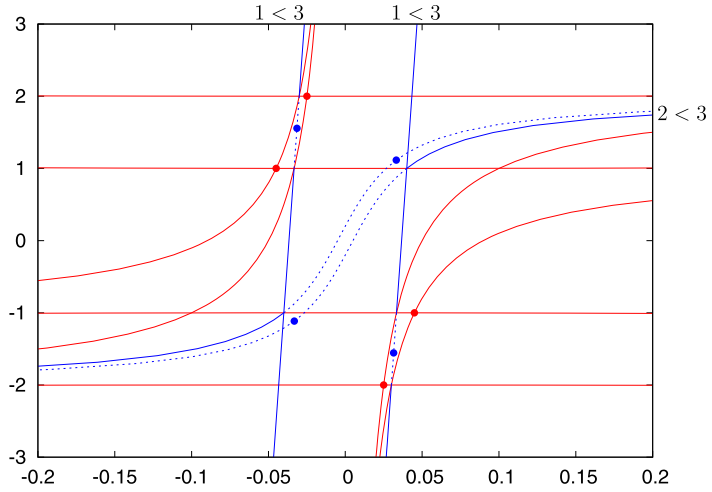

Fig. 3. Stokes geometry for Example 1 with $\epsilon_1 = 0.09$ and $\epsilon_2 = 0.1$.

point near $2i$. Then we find that it goes through the turning point near i seeing it on the left-hand side when $\epsilon_1 \leq 0.06$ and on the right-hand side when $\epsilon_1 \geq 0.07$. This means that at some value between 0.06 and 0.07 the Stokes curve hits the turning point. If the turning point is simple, such a degenerate situation is studied in [1]. One of our main concerns in this paper is what happens if a Stokes curve hits a double turning point and what kind of influence it has on the continuation problem of solutions.

Now let us briefly explain our original motivation to study the example. Take suitably normalized WKB solutions $(\Psi^{(1)}, \Psi^{(2)}, \Psi^{(3)})$ of the form

$$\Psi^{(j)} = \eta^{-\frac{1}{2}} \exp\left(\frac{\eta}{i} \int_{t_0}^{t} \rho_j(s) ds + \frac{1}{i} \int_{t_0}^{t} \left(\frac{|c_{jk}|^2}{\rho_j - \rho_k} + \frac{|c_{jl}|^2}{\rho_j - \rho_l} \right) ds \right) \times \left(e^{(j)} + O(\eta^{-\frac{1}{2}}) \right). \tag{3}$$

Introduce other fundamental systems of solutions

$$\Psi^{\pm,(j)} = \Psi^{(j)} N^{\pm,(j)} \tag{4}$$

with normalization factors $N^{\pm,(j)}$ so that

$$\lim_{t \to \pm\infty} \left| \Psi^{\pm,(j)}(t) \right| = e^{(j)} \quad (j = 1, 2, 3), \tag{5}$$

where $e^{(j)}$'s are unit vectors

$$e^{(1)} = {}^{\mathrm{t}}(1, 0, 0), \quad e^{(2)} = {}^{\mathrm{t}}(0, 1, 0), \quad e^{(3)} = {}^{\mathrm{t}}(0, 0, 1). \tag{6}$$

Letting M be the connection matrix for the WKB solutions $(\Psi^{(1)}, \Psi^{(2)}, \Psi^{(3)})$ from $-\infty$ to $+\infty$, we define the S-matrix

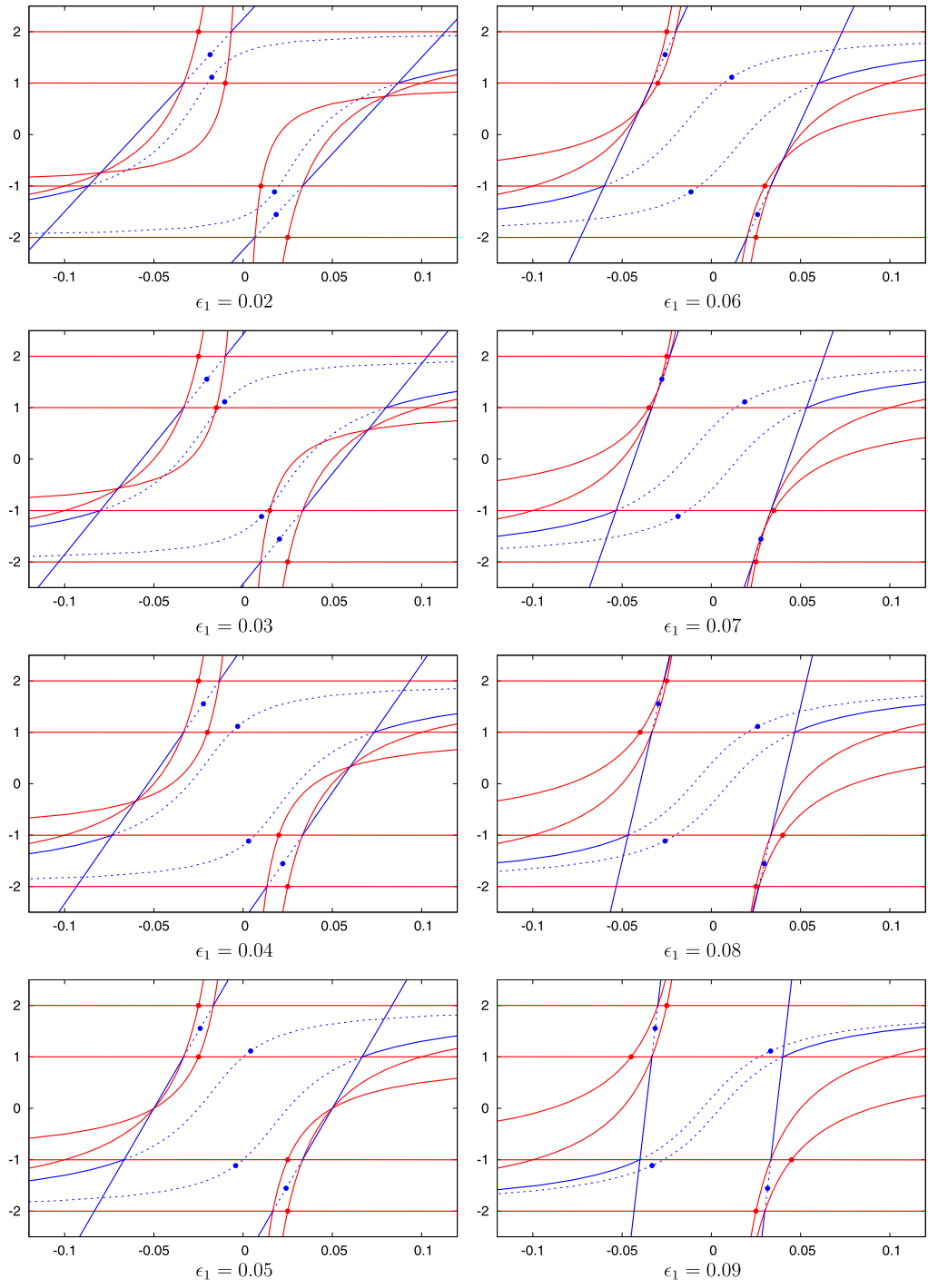

Fig. 4. Change of Stokes geometry for Example 1 as $\epsilon_1 = 0.02 \to 0.09$ with $\epsilon_2 = 0.1$.

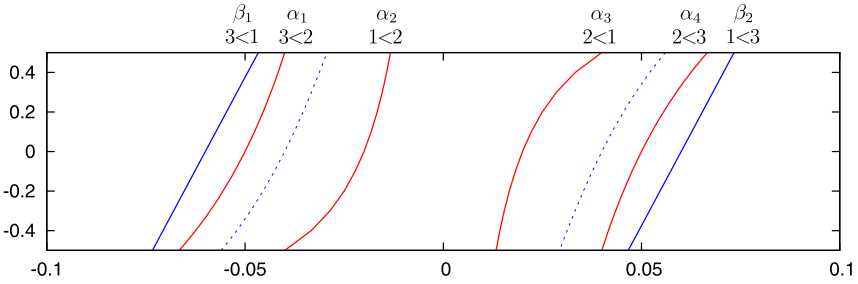

Fig. 5. Stokes curves near the real axis for Example 1 with $\epsilon_1 = 0.02$ and $\epsilon_2 = 0.1$.

$$S = \begin{pmatrix} N^{+,(1)} & & \\ & N^{+,(2)} & \\ & & N^{+,(3)} \end{pmatrix}^{-1} M \begin{pmatrix} N^{-,(1)} & & \\ & N^{-,(2)} & \\ & & N^{-,(3)} \end{pmatrix}. \tag{7}$$

The squared modulus of each element of S represents the transition probability. In many cases, $N^{\pm,(j)}$ can be taken as $1+O(\eta^{-1/2})$. We first consider the case $\epsilon_1 = 0.02$. There are six active Stokes curves crossing the real axis, and we let α_1, α_2, α_3, α_4 and β_1, β_2 denote the Stokes coefficients attached to the Stokes curves as shown in Fig. 5. For example, we assign α_1 the second Stokes curve from the left, i.e., the Stokes curve of type $3 < 2$. This means that, as the independent variable t goes across the curve from left to right, the WKB solutions change as $(\Psi^{(1)}, \Psi^{(2)}, \Psi^{(3)}) \mapsto (\Psi^{(1)}, \Psi^{(2)} + \alpha_1\Psi^{(3)}, \Psi^{(3)})$. Then the analytic continuation of WKB solutions from $-\infty$ to $+\infty$ is given by $(\Psi^{(1)}, \Psi^{(2)}, \Psi^{(3)}) \mapsto (\Psi^{(1)}, \Psi^{(2)}, \Psi^{(3)})M$ with the connection matrix

$$M = \begin{pmatrix} 1+\beta_1\beta_2 & \alpha_2+\alpha_1\beta_2 & \beta_2 \\ \alpha_3+\alpha_4\beta_1 & 1+\alpha_2\alpha_3+\alpha_1\alpha_4 & \alpha_4 \\ \beta_1 & \alpha_1 & 1 \end{pmatrix}. \tag{8}$$

The probability of transition $j \to k$ is given by the squared absolute value of (k, j)-element. As we shall see later, $(1, 3)$-element β_2 is much bigger than $(2, 3)$-element α_4. Furthermore, the transition $3 \to 1$ is caused by a virtual turning point (or new Stokes curve), whereas the transition $3 \to 2$ is caused by an ordinary turning point (or ordinary Stokes curve). Thus the transition caused by a virtual turning point is much bigger than the transition caused by an ordinary turning point in the case of Example 1; this is the motivation we study this example.

Meanwhile, as we have already observed, a Stokes curve hits a double turning point at some value of ϵ_1 between 0.06 and 0.07 and the configuration of Stokes curves differs between $\epsilon_1 = 0.02$ and $\epsilon_1 = 0.09$ (cf. Figs. 2 and 3). As its consequence, the explicit form of the connection matrix changes as

$$\hat{M} = \begin{pmatrix} 1+\hat{\beta}_1\hat{\beta}_2 & \hat{\alpha}_2+(\hat{\alpha}_1+\hat{\alpha}_2\hat{\beta}_1)\hat{\beta}_2 & \hat{\beta}_2 \\ \hat{\alpha}_3+(\hat{\alpha}_4+\hat{\alpha}_3\hat{\beta}_2)\hat{\beta}_1 & 1+\hat{\alpha}_2\hat{\alpha}_3+(\hat{\alpha}_1+\hat{\alpha}_2\hat{\beta}_1)(\hat{\alpha}_4+\hat{\alpha}_3\hat{\beta}_2) & \hat{\alpha}_4+\hat{\alpha}_3\hat{\beta}_2 \\ \hat{\beta}_1 & \hat{\alpha}_1+\hat{\alpha}_2\hat{\beta}_1 & 1 \end{pmatrix} \tag{9}$$

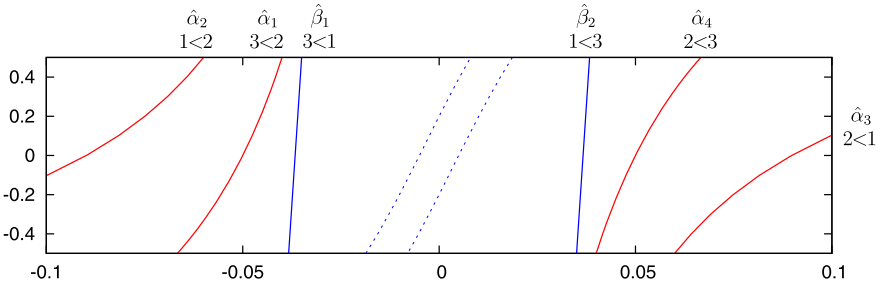

Fig. 6. Stokes curves near the real axis for Example 1 with $\epsilon_1 = 0.09$ and $\epsilon_2 = 0.1$.

when $\epsilon_1 = 0.09$ (cf. §3). Here we assign the symbols $\hat{\alpha}_j$'s and $\hat{\beta}_k$'s the Stokes coefficients in a way consistent with the case $\epsilon_1 = 0.02$ (Fig. 6), that is, α_j and $\hat{\alpha}_j$ are attached to the ordinary Stokes curves emanating from the same ordinary turning point and β_k and $\hat{\beta}_k$ are attached to the new Stokes curves emanating from the same virtual turning point. Then, looking at $(2,3)$-element for example, we see a new term $\hat{\alpha}_3\hat{\beta}_2$ appears. As we see later, $\hat{\alpha}_4$ and $\hat{\alpha}_3\hat{\beta}_2$ have the same order of magnitude (cf. Remark 3 in §3.1). Thus a simple-minded comparison might lead to a conclusion that the connection matrix changes discontinuously by a small change of ϵ_1. However it is not the case. To discuss the transition probability and the influence of virtual turning points on it in a neat manner, we need to examine what happens if a Stokes curve hits a double turning point. Thus the aim of this paper is twofold, namely, to analyze a phenomenon that the effect of virtual turning points may become bigger than that of ordinary turning points on one hand, and to examine a bifurcation phenomenon of Stokes curves around a double turning point on the other hand.

The construction of this paper is as follows. First in §2 we study a bifurcation phenomenon of Stokes curves around a double turning point, which is observed when a Stokes curve hits a double turning point. Then in §3 we apply the results in §2 to two examples, one of which is Example 1 above, and discuss the influence of virtual turning points on the transition probabilities in the examples.

The author would like to thank Professor Yoshitsugu Takei for his advice and many useful comments. Special gratitude is also due to Professor Takahiro Kawai for his persistent encouragement and valuable comments.

2. Bifurcation of Stokes curves around a double turning point

We consider the system (1) with a parameter a:

$$H(t,a,\eta) = H_0(t,a) + \eta^{-1/2}H_{1/2} = \begin{pmatrix} \rho_1(t,a) & 0 & 0 \\ 0 & \rho_2(t,a) & 0 \\ 0 & 0 & \rho_3(t,a) \end{pmatrix} + \eta^{-1/2}\begin{pmatrix} 0 & c_{12} & c_{13} \\ \overline{c_{12}} & 0 & c_{23} \\ \overline{c_{13}} & \overline{c_{23}} & 0 \end{pmatrix}, \tag{10}$$

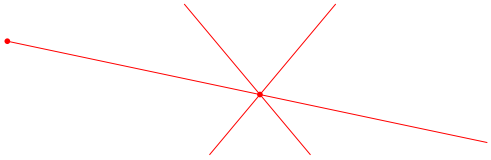

Fig. 7. A Stokes curve hits a double turning point.

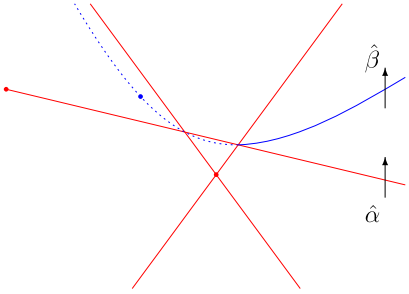

Fig. 8. Stokes geometry for $a = a_{-1}$.

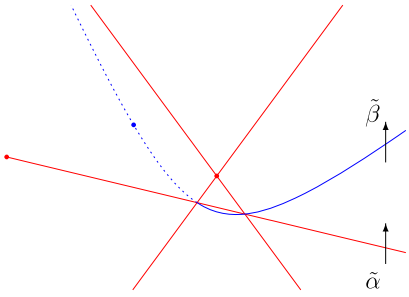

Fig. 9. Stokes geometry for $a = a_1$.

where ρ_j's are assumed to be holomorphic in a. (ρ_j's are not necessarily real polynomials.) System (1) has double turning points, and we assume that a Stokes curve hits a double turning point at $a = a_0$ (Fig. 7). To be more specific, we assume that the Stokes geometry changes from Fig. 8 to Fig. 9 as the parameter a moves from a_{-1} to a_1 near $a = a_0$. Under this geometric setting we will show that the Stokes coefficients do not change discontinuously, namely $\tilde{\alpha} = \hat{\alpha}$ and $\tilde{\beta} = \hat{\beta}$. We verify this by employing two fundamental techniques: one is the transformation near a double turning point to the canonical equation, and the other is a technique to determine Stokes coefficients at an ordered crossing point based on the single-valuedness of solutions at the crossing point (cf. [4,2,3]). In the following we call the latter technique "the principle (for determining Stokes coefficients) at an ordered crossing point".

First we recall the transformation near a double turning point to the canonical form established in [3]. Let t_0 be a double turning point. Without loss of generality, we may assume that the double turning point is of type $(1, 2)$, that is, $\rho_1(t_0) = \rho_2(t_0)$ holds.

It is shown in [3, Appendix] (cf. also [10, Theorems 3.3.1 and 3.3.2]) that there exists a formal transformation

$$\Psi = \exp(\eta f(t))T(z,\eta)\Phi \tag{11}$$

which transforms the equation (1) with (2) to the canonical one near $t = t_0$, where

$$T(z,\eta) = T_0(z) + \eta^{-1/2}T_{1/2}(z) + \eta^{-1}T_1(z) + \cdots, \tag{12}$$

$$f(t) = \frac{1}{2i}\int_{t_0}^{t} (\rho_1(s) + \rho_2(s))\, ds \tag{13}$$

and

$$z = \left(\pm \int_{t_0}^{t} (\rho_1(s) - \rho_2(s))\, ds \right)^{1/2}. \tag{14}$$

The canonical equation is given by

$$i\frac{d}{dz}\Phi = \eta \begin{pmatrix} G & \\ & g \end{pmatrix} \Phi, \tag{15}$$

where

$$\begin{aligned} G = G(z,\eta) &= \begin{pmatrix} -z & 0 \\ 0 & z \end{pmatrix} + \eta^{-1/2} \begin{pmatrix} 0 & \mu(\eta) \\ \nu(\eta) & 0 \end{pmatrix}, \\ g = g(z,\eta) &= g_0(z) + \eta^{-1/2}g_{1/2}(z) + \cdots \end{aligned} \tag{16}$$

with $\mu(\eta) = \mu_0 + \eta^{-1/2}\mu_{1/2} + \cdots$ and $\nu(\eta) = \nu_0 + \eta^{-1/2}\nu_{1/2} + \cdots$. All the entries above, i.e., $T_{j/2}(z)$ and $g_{k/2}(z)$ are holomorphic near the turning point $t = t_0$. Note that in [3] the case where the equation (1) contains a parameter is not discussed. By exactly the same manner, we can deal with the equation (1) with (10), that is, the case where the equation depends on a parameter. In parallel to the above result, we can find a transformation

$$\Psi = \exp(\eta f(t,a))T(z,a,\eta)\Phi \tag{17}$$

which transforms the equation (1) with (10) to its canonical form near $t = t_0$, where

$$T(z,a,\eta) = T_0(z,a) + \eta^{-1/2}T_{1/2}(z,a) + \eta^{-1}T_1(z,a) + \cdots, \tag{18}$$

$$f(t,a) = \frac{1}{2i}\int_{t_0(a)}^{t} (\rho_1(s,a) + \rho_2(s,a))\, ds \tag{19}$$

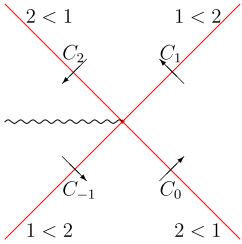

Fig. 10. Stokes curves of the canonical equation and Stokes coefficients.

and

$$z = \left(\pm \int_{t_0(a)}^{t} (\rho_1(s,a) - \rho_2(s,a))\, ds \right)^{1/2}. \tag{20}$$

The canonical form is again given by (15) with

$$\begin{aligned} G = G(z,a,\eta) &= \begin{pmatrix} -z & 0 \\ 0 & z \end{pmatrix} + \eta^{-1/2} \begin{pmatrix} 0 & \mu(a,\eta) \\ \nu(a,\eta) & 0 \end{pmatrix}, \\ g = g(z,a,\eta) &= g_0(z,a) + \eta^{-1/2} g_{1/2}(z,a) + \cdots. \end{aligned} \tag{21}$$

Here $\mu(a,\eta) = \mu_0(a) + \eta^{-1/2}\mu_{1/2}(a) + \cdots$ and $\nu(a,\eta) = \nu_0(a) + \eta^{-1/2}\nu_{1/2}(a) + \cdots$, and all the entries $T_{j/2}(z,a)$, $\mu_{k/2}(a)$, $\nu_{k/2}(a)$ and $g_{k/2}(z,a)$ depend holomorphically on a. This canonical equation has a good couple of linearly independent solutions $\Phi^{(1)}(z,a)$ and $\Phi^{(2)}(z,a)$ [10, (3.3.18), (3.3.20) and (3.3.21)]:

$$\begin{aligned} \Phi^{(1)}(z,a) &= \eta^{-1/2} e^{i\eta z^2/2} z^{i\mu\nu/2} \begin{pmatrix} 1 + \cdots \\ \frac{-\eta^{-1/2}\nu_0}{2z} + \cdots \\ 0 \end{pmatrix}, \\ \Phi^{(2)}(z,a) &= \eta^{-1/2} e^{-i\eta z^2/2} z^{-i\mu\nu/2} \begin{pmatrix} \frac{\eta^{-1/2}\mu_0}{2z} + \cdots \\ 1 + \cdots \\ 0 \end{pmatrix} \end{aligned} \tag{22}$$

for which the Stokes coefficients C_{-1}, C_0, C_1 and C_2 in Fig. 10 are given by

$$\begin{aligned} C_{-1} &= \frac{(2\eta)^{i\mu\nu/2}\mu\sqrt{\pi}}{\Gamma(i\mu\nu/2+1)} e^{5i\pi/4} e^{-3\pi\mu\nu/4}, & C_0 &= \frac{(2\eta)^{-i\mu\nu/2}\nu\sqrt{\pi}}{\Gamma(-i\mu\nu/2+1)} e^{-i\pi/4} e^{\pi\mu\nu/4}, \\ C_1 &= \frac{(2\eta)^{i\mu\nu/2}\mu\sqrt{\pi}}{\Gamma(i\mu\nu/2+1)} e^{i\pi/4} e^{\pi\mu\nu/4}, & C_2 &= \frac{(2\eta)^{-i\mu\nu/2}\nu\sqrt{\pi}}{\Gamma(-i\mu\nu/2+1)} e^{3i\pi/4} e^{-3\pi\mu\nu/4}. \end{aligned} \tag{23}$$

Here $\Gamma(\cdot)$ denotes Euler's gamma function. For example, as the variable z traverses counterclockwise the Stokes curve in the fourth quadrant, the solutions change as $(\Phi^{(1)}, \Phi^{(2)}) \mapsto (\Phi^{(1)} + C_0\Phi^{(2)}, \Phi^{(2)})$. We note that a branch cut for the WKB so-

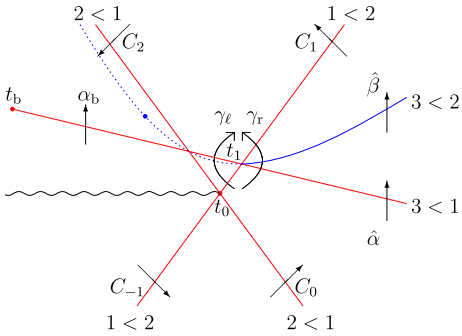

Fig. 11. Stokes coefficients for $a = a_{-1}$.

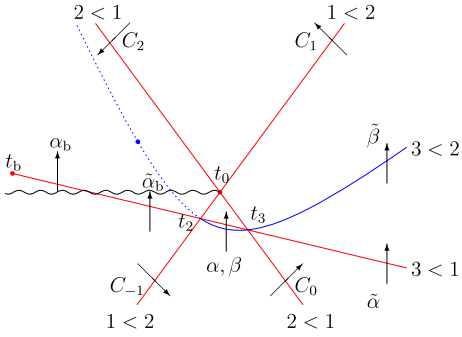

Fig. 12. Stokes coefficients for $a = a_1$.

lutions is needed due to the factor $z^{\pm i\mu\nu/2}$. Taking another independent solution $\Phi^{(3)}(z,a) = \eta^{-1/2}\exp[(\eta/i)\int_{z_0}^{z} g(z,a,\eta)\,dz]e^{(3)}$, we fix a triplet of WKB solutions $\Psi^{(j)} = \exp(\eta f)T\Phi^{(j)}$ $(j = 1,2,3)$. We remark that $\Psi^{(1)}$ and $\Psi^{(2)}$ inherit their Stokes coefficients C_{-1}, C_0, C_1 and C_2 from $\Phi^{(1)}$ and $\Phi^{(2)}$. That is, $(\Psi^{(1)}, \Psi^{(2)}) \mapsto (\Psi^{(1)} + C_0\Psi^{(2)}, \Psi^{(2)})$ holds with the same constant C_0 as t traverses counterclockwise the corresponding Stokes curve, etc.

Remark 1. Although we do not discuss the summability of the formal transformation in this paper, the above connection formula $(\Psi^{(1)}, \Psi^{(2)}) \mapsto (\Psi^{(1)} + C_0\Psi^{(2)}, \Psi^{(2)})$ etc. for $\Psi^{(j)}$ naturally follows once the summability of the formal transformation is confirmed.

Now we compute the Stokes coefficients after the bifurcation of Stokes curves around a double turning point occurs and the configuration changes from Fig. 8 (or Fig. 11) to Fig. 9 (or Fig. 12). Our goal is to show the following.

Theorem 1. *Under the setting above, the following hold:*

$$\begin{aligned} \tilde{\alpha} &= \hat{\alpha}, & \alpha &= \hat{\alpha} + C_0\hat{\beta}, \\ \tilde{\beta} &= \hat{\beta}, & \beta &= \hat{\beta}. \end{aligned} \tag{24}$$

We are going to calculate the Stokes coefficients $\hat{\alpha}$, $\hat{\beta}$, α, β and $\tilde{\alpha}$, $\tilde{\beta}$ step by step. For $a = a_{-1}$, we apply the "principle" at the ordered crossing point t_1 to determine $\hat{\alpha}$ and $\hat{\beta}$. We shall here demonstrate it in an explicit manner. (See [10, Recipe 1.5.1 (R.v)] for details.) Let α_{b} denote the Stokes coefficient for the Stokes curve emanating from the turning point t_{b}. We first note that at an ordered crossing point with types $j > k$, $k > l$ and $j > l$, only the Stokes curve of type $j > l$ changes its Stokes coefficient at the crossing point. Therefore we obtain

$$\hat{\alpha} = \alpha_{\mathrm{b}}. \tag{25}$$

We next calculate the change of Stokes coefficients for the Stokes curve of type $j > l$ at an ordered crossing point, namely $\hat{\beta}$ in this case. For that purpose, we analytically continue $\Psi^{(2)}$ along two paths γ_ℓ and γ_{r} (Fig. 11). Along γ_{r} we have

$$\Psi^{(2)} \mapsto \Psi^{(2)} + C_1\Psi^{(1)} + \hat{\beta}\Psi^{(3)}, \tag{26}$$

and along γ_ℓ

$$\Psi^{(2)} \mapsto \Psi^{(2)} + C_1\Psi^{(1)} + C_1\alpha_{\mathrm{b}}\Psi^{(3)}. \tag{27}$$

Since the point t_1 is a regular point of the equation, these two results should coincide. Therefore by comparison we obtain

$$\hat{\beta} = C_1\alpha_{\mathrm{b}}. \tag{28}$$

For $a = a_1$, we first need to determine the Stokes coefficient $\tilde{\alpha}_{\mathrm{b}}$ (Fig. 12), in other words, to see how WKB solutions change as z crosses over the branch cut from left to right. Since $\Phi^{(1)}$ has the factor $z^{i\mu\nu/2}$, across the cut we have

$$\Phi^{(1)}(e^{2\pi i}z) = e^{-\pi\mu\nu}\Phi^{(1)}(z). \tag{29}$$

The same holds for $\Psi^{(1)}$. On the other hand, $\Psi^{(3)}$ is holomorphic at the double turning point, and so it does not change across the cut. These mean

$$\tilde{\alpha}_{\mathrm{b}} = e^{\pi\mu\nu}\alpha_{\mathrm{b}}. \tag{30}$$

Then we apply the "principle" for the Stokes coefficients at t_2 (Fig. 12) to obtain

$$\alpha = \tilde{\alpha}_{\mathrm{b}} \tag{31}$$

$$= e^{\pi\mu\nu}\alpha_{\mathrm{b}}. \tag{32}$$

$$\beta = -C_{-1}\alpha \tag{33}$$

$$= -e^{\pi\mu\nu}C_{-1}\alpha_{\mathrm{b}}. \tag{34}$$

In order, relying on the "principle" at t_3 (Fig. 12), we have

$$\tilde{\alpha} = \alpha - C_0\tilde{\beta} \tag{35}$$

$$= e^{\pi\mu\nu}(1 + C_{-1}C_0)\alpha_{\mathrm{b}}, \tag{36}$$

$$\tilde{\beta} = \beta \tag{37}$$

$$= -e^{\pi\mu\nu}C_{-1}\alpha_{\mathrm{b}}. \tag{38}$$

Now, using (23) and recalling the well known formulas for the gamma function

$$\Gamma(X+1) = X\Gamma(X), \quad \frac{\pi}{\Gamma(X)\Gamma(1-X)} = \sin(\pi X), \tag{39}$$

we confirm $\tilde{\alpha} = \hat{\alpha}$ and $\tilde{\beta} = \hat{\beta}$. We emphasize that the explicit form (23) of the Stokes coefficients around a double turning point is essential here. Using (35) and (37), we obtain $\alpha = \hat{\alpha} + C_0\hat{\beta}$ and $\beta = \hat{\beta}$ as well. This completes the proof of Theorem 1.

3. Non-adiabatic transition probability and effect of virtual turning points

In this section, we discuss influence of virtual turning points and new Stokes curves on the transition probabilities through examples. In §3.1, we concretely discuss the influence in Example 1. We compare absolute values of two elements of the connection matrix, one of which is due to an ordinary turning point and the other is due to a virtual turning point. That is, we make a comparison between effect of an ordinary turning point and that of a virtual turning point in two matrix elements. We see that a virtual turning point has bigger influence on the transition probabilities. Then in §3.2 we present another example, where an element of the connection matrix has two terms, one of which is due to an ordinary turning point and the other is due to a virtual turning point. For this example we can make a comparison within a single matrix element and again we find that a virtual turning point has bigger influence.

3.1. Comparison in two matrix elements

We start with re-examining the change of Stokes geometry of Example 1 (Fig. 4). Since each Stokes geometry is symmetric with respect to the origin, we look at only the left-half part. Focusing our attention on the vicinity of the real axis, we first see that when $\epsilon_1 \simeq 0.05$, a crossing point of two ordinary Stokes curves and a new Stokes curve comes on the axis. Then at some value between 0.06 and 0.07, a Stokes curve from a turning point near $2i$ meets another turning point near i. Therefore the transition of the Stokes geometry between $\epsilon_1 = 0.02$ and $\epsilon_1 = 0.09$ has three phases. We display them in Fig. 13. The arrows represent the real axes, namely the paths along which we analytically continue the solutions. Comparing this with the geometry for Theorem 1 (Fig. 14), we readily see that analytic continuations with $\epsilon_1 = 0.09$, 0.06 and 0.02 correspond to those

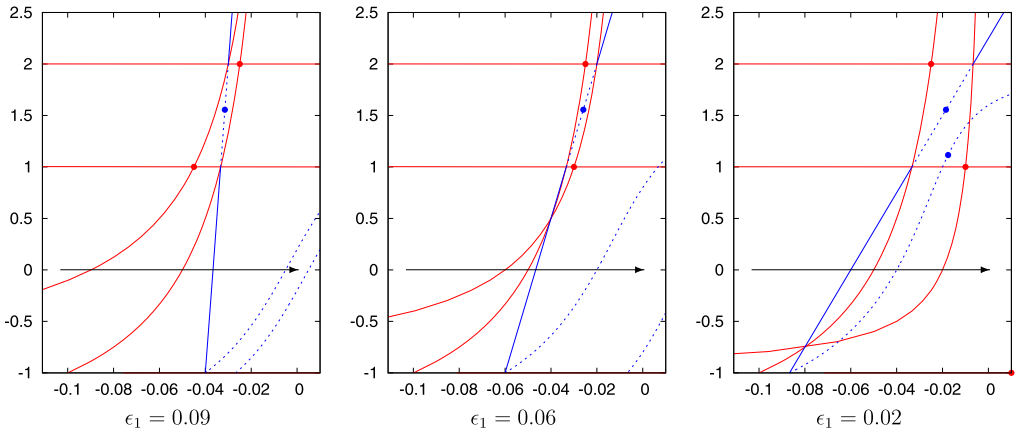

Fig. 13. A part of the Stokes geometry of Example 1 with $\epsilon_1 = 0.09$, 0.06 and 0.02.

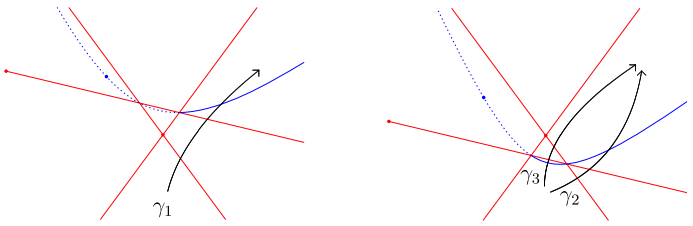

Fig. 14. Stokes geometry for Theorem 1.

along γ_1, γ_2 and γ_3 respectively. At the same time, the connection matrices M and $\hat{M}$ given in (8) and (9) can be written as

$$M = M_{\mathrm{r}} M_{\ell}, \tag{40}$$

$$\hat{M} = \hat{M}_{\mathrm{r}} \hat{M}_{\ell} \tag{41}$$

with

$$M_{\ell} = \begin{pmatrix} 1 & \alpha_2 & 0 \\ 0 & 1 & 0 \\ \beta_1 & \alpha_1 & 1 \end{pmatrix}, \quad M_{\mathrm{r}} = \begin{pmatrix} 1 & 0 & \beta_2 \\ \alpha_3 & 1 & \alpha_4 \\ 0 & 0 & 1 \end{pmatrix}, \tag{42}$$

$$\hat{M}_{\ell} = \begin{pmatrix} 1 & \hat{\alpha}_2 & 0 \\ 0 & 1 & 0 \\ \hat{\beta}_1 & \hat{\alpha}_1 + \hat{\alpha}_2 \hat{\beta}_1 & 1 \end{pmatrix}, \quad \hat{M}_{\mathrm{r}} = \begin{pmatrix} 1 & 0 & \hat{\beta}_2 \\ \hat{\alpha}_3 & 1 & \hat{\alpha}_4 + \hat{\alpha}_3 \hat{\beta}_2 \\ 0 & 0 & 1 \end{pmatrix}. \tag{43}$$

M_{ℓ} and $\hat{M}_{\ell}$ are the connection matrices from $-\infty$ to 0, and M_{r} and $\hat{M}_{\mathrm{r}}$ are the connection matrices from 0 to $+\infty$. Comparing the difference between (42) and (43) with Theorem 1, we see that $M = \hat{M}$, except for the fact that M and $\hat{M}$ are connection matrices for WKB solutions (3) while Theorem 1 treats of those normalized at a double turning point. Here, WKB solutions normalized at a double turning point mean those defined through the

transformation near a double turning point discussed in §2. In the following we discuss this gap. To be concrete, we show that

$$M_\ell = \hat{M}_\ell, \quad M_{\mathrm{r}} = \hat{M}_{\mathrm{r}} \tag{44}$$

hold.

Let $(\Psi^{(1)}, \Psi^{(2)}, \Psi^{(3)})$ be WKB solutions (3), which are used for the computation of M and $\hat{M}$, and $(\Psi^{\ell,(1)}, \Psi^{\ell,(2)}, \Psi^{\ell,(3)})$ be WKB solutions normalized at the double turning point near $t = i$. We assign M_ℓ^ℓ and $\hat{M}_\ell^\ell$ the connection matrices for $(\Psi^{\ell,(1)}, \Psi^{\ell,(2)}, \Psi^{\ell,(3)})$ from $-\infty$ to 0 with $\epsilon_1 = 0.02$ and $\epsilon_1 = 0.09$ respectively. As we have checked above,

$$M_\ell^\ell = \hat{M}_\ell^\ell \tag{45}$$

holds. With $\epsilon = (\epsilon_1, \epsilon_2)$, since $\Psi^{(j)}(t,\epsilon)$'s are of the form

$$\Psi^{(j)}(t,\epsilon) = \exp\left(\frac{\eta}{i}\int_{t_0}^{t} \rho_j(s,\epsilon)\,ds\right)\sum_{m=0}^{\infty}\Psi_{m/2}^{(j)}(t,\epsilon)\eta^{-(m+1)/2} \qquad (j=1,2,3) \tag{46}$$

and $\Psi^{\ell,(j)}(t,\epsilon)$'s are of the form

$$\Psi^{\ell,(j)}(t,\epsilon) = \exp\left(\frac{\eta}{i}\int_{i\sqrt{1+i\epsilon_1}}^{t} \rho_j(s,\epsilon)\,ds\right)\sum_{m=0}^{\infty}\Psi_{m/2}^{\ell,(j)}(t,\epsilon)\eta^{-(m+1)/2} \qquad (j=1,2), \tag{47}$$

$$\Psi^{\ell,(3)}(t,\epsilon) = \exp\left(\frac{\eta}{i}\int_{t_0}^{t} \rho_3(s,\epsilon)\,ds\right)\sum_{m=0}^{\infty}\Psi_{m/2}^{\ell,(3)}(t,\epsilon)\eta^{-(m+1)/2}, \tag{48}$$

these two triplets of solutions are related by

$$\Psi^{(j)} = \Psi^{\ell,(j)} l^{\ell,(j)} \tag{49}$$

with

$$l^{\ell,(1)}(\epsilon,\eta) = \exp\left(\frac{\eta}{i}\int_{t_0}^{i\sqrt{1+i\epsilon_1}} \rho_1(t,\epsilon)\,dt\right)\left(l_0^{\ell,(1)}(\epsilon) + \eta^{-1/2} l_{1/2}^{\ell,(1)}(\epsilon) + \cdots\right), \tag{50}$$

$$l^{\ell,(2)}(\epsilon,\eta) = \exp\left(\frac{\eta}{i}\int_{t_0}^{i\sqrt{1+i\epsilon_1}} \rho_2(t,\epsilon)\,dt\right)\left(l_0^{\ell,(2)}(\epsilon) + \eta^{-1/2} l_{1/2}^{\ell,(2)}(\epsilon) + \cdots\right), \tag{51}$$

$$l^{\ell,(3)}(\epsilon,\eta) = \left(l_0^{\ell,(3)}(\epsilon) + \eta^{-1/2} l_{1/2}^{\ell,(3)}(\epsilon) + \cdots\right). \tag{52}$$

Because the transformation at a double turning point is holomorphic in ϵ, the entries above are also holomorphic in ϵ. Therefore, defining $L^\ell = \mathrm{diag}(l^{\ell,(1)}, l^{\ell,(2)}, l^{\ell,(3)})$,

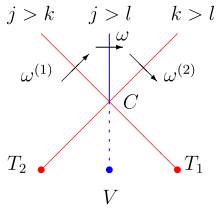

Fig. 15. A new Stokes curve emanating from V passes through an ordered crossing point C of two ordinary Stokes curves emanating from T_1 and T_2; ω, $\omega^{(1)}$ and $\omega^{(2)}$ denote the Stokes coefficients attached to them.

$$M_\ell = (L^\ell)^{-1} M_\ell^\ell L^\ell, \tag{53}$$

$$\hat{M}_\ell = (L^\ell)^{-1} \hat{M}_\ell^\ell L^\ell \tag{54}$$

hold. Combining with (45), we obtain $M_\ell = \hat{M}_\ell$. $M_{\mathrm{r}} = \hat{M}_{\mathrm{r}}$ is shown by the same manner.

Remark 2. Though we do not present here the connection matrix for $\epsilon_1 = 0.06$, in view of Figs. 13, 14 and Theorem 1, it equals M and $\hat{M}$.

Now we discuss magnitude of connection matrix elements, which we touched upon in Introduction. First we recall the concrete form of Stokes coefficients. For the later reference we present formulas in a general setting. For WKB solutions of the form

$$\Psi^{(j)}(t,\epsilon) = \exp\left(\frac{\eta}{i}\int_{t_0}^{t} \rho_j(s)\,ds\right) \sum_{m=0}^{\infty} \Psi_{m/2}^{(j)}(t,\epsilon)\eta^{-(m+1)/2} \qquad (j=1,2,3), \tag{55}$$

and for an ordinary Stokes curve of type $j < k$ emanating from a double turning point T, the Stokes coefficient ω is given by

$$\omega = \omega_0(\eta) \exp\left[\frac{\eta}{i}\int_{T}^{t_0} (\rho_j - \rho_k)\,dt\right]. \tag{56}$$

Here ω_0 does not contain an exponential factor with respect to η. See [10, (3.3.31)] for its complete form. We next consider the Stokes coefficient attached to a new Stokes curve. Let us consider the situation shown in Fig. 15, that is, two ordinary Stokes curves with Stokes coefficients $\omega^{(1)}$ and $\omega^{(2)}$ make an ordered crossing point C and it induces a new Stokes curve emanating from a virtual turning point V. Then, as is verified in §2 (cf. (28)), the Stokes coefficient ω of the new Stokes curve is given by

$$\omega = \omega^{(1)}\omega^{(2)} \tag{57}$$

$$= \omega_0^{(1)}\omega_0^{(2)} \exp\left[\frac{\eta}{i}\left\{\int_{T_1}^{t_0} (\rho_j - \rho_k)\,dt + \int_{T_2}^{t_0} (\rho_k - \rho_l)\,dt\right\}\right]. \tag{58}$$

Moreover, the sum of the two integrals in the right-hand side of (58) is represented by a single integral from the virtual turning point V [10, (3.2.6)]:

$$\omega = \omega_0^{(1)}\omega_0^{(2)} \exp\left[\frac{\eta}{i}\int_V^{t_0} (\rho_j - \rho_l)\, dt\right]. \tag{59}$$

Having these formulas for the Stokes coefficients in mind, we look back to (1,3)- and (2,3)-elements of the connection matrix M. With $v(\simeq 0.0185 - 1.5557i)$ being the virtual turning point, the exponential factor of β_2 is

$$\begin{aligned}&\exp\left[\frac{\eta}{i}\int_v^{t_0} (\rho_1 - \rho_3)\, dt\right]\\ &\quad = \exp\left[\frac{\eta}{i}\left\{\int_{-2i\sqrt{1+(i\epsilon_2/4)}}^{t_0} (\rho_2 - \rho_3)\, dt + \int_{-i\sqrt{1+i\epsilon_1}}^{t_0} (\rho_1 - \rho_2)\, dt\right\}\right],\end{aligned} \tag{60}$$

and that of α_4 is

$$\exp\left[\frac{\eta}{i}\int_{-2i\sqrt{1+(i\epsilon_2/4)}}^{t_0} (\rho_2 - \rho_3)\, dt\right]. \tag{61}$$

Since the real part of $(\eta/i)\int_{-i\sqrt{1+i\epsilon_1}}^{t_0}(\rho_1 - \rho_2)\, dt$ is positive, $|\beta_2|$ is much bigger than $|\alpha_4|$. Thus the transition $3 \to 1$, which can be interpreted as an effect of the virtual turning point v, is much bigger than the transition $3 \to 2$, which can be interpreted as an effect of the ordinary turning point at $-2i\sqrt{1 + (i\epsilon_2/4)}$.

Remark 3. As for $\hat{M}$, noting that the exponential factor of $\hat{\alpha}_3$ is

$$\exp\left[\frac{\eta}{i}\int_{-i\sqrt{1+i\epsilon_1}}^{t_0} (\rho_2 - \rho_1)\, dt\right], \tag{62}$$

$\hat{\alpha}_4$ and $\hat{\alpha}_3\hat{\beta}_2$ have the same exponential factor

$$\exp\left[\frac{\eta}{i}\int_{-2i\sqrt{1+(i\epsilon_2/4)}}^{t_0} (\rho_2 - \rho_3)\, dt\right]. \tag{63}$$

Therefore the two terms of (2,3)-element have the same exponential factor. This is the reason why the apparent difference between α_4 and $\hat{\alpha}_4 + \hat{\alpha}_3\hat{\beta}_2$ seems crucial. The calcu-

lation above with Theorem 1 shows that the difference of (2,3)-elements of M and $\hat{M}$ is only apparent, and that $\alpha_4 = \hat{\alpha}_4 + \hat{\alpha}_3\hat{\beta}_2$ actually holds.

3.2. Comparison within a single matrix element

In this subsection we treat the following example:

Example 2. $\rho_1(t) = t^2 + 1 + i\epsilon_1$, $\rho_2(t) = 0$ and $\rho_3(t) = 2(t^2 + 4 + i\epsilon_2)$.

This is different from Example 1 by the factor 2 in ρ_3, and has two additional ordinary turning points at $\pm\sqrt{7}i\sqrt{1 + i(2\epsilon_2 - \epsilon_1)/7}$. We first study how the Stokes geometry changes as ϵ_1 moves from 0.02 to 0.07 with $\epsilon_2 = 0.1$ fixed. In Fig. 16, Stokes geometries with $\epsilon_1 = 0.02$, 0.0525, 0.06 and 0.07 are given. Stokes curves near the real axis are given in Fig. 17. We first see that before $\epsilon_1 = 0.0525$ a crossing point A_1 (Fig. 17 (b)) of three Stokes curves traverses the real axis upward. This move of a crossing point is exactly what we observed in Example 1 near $\epsilon_1 \simeq 0.05$. In the present example, there exists another crossing point A_0 (Fig. 17 (b)) of three Stokes curves, one of which is an ordinary Stokes curve emanating from the turning point near $\sqrt{7}i$. Such a crossing point does not appear in Example 1. This crossing point also traverses the real axis upward as ϵ_1 increases (Fig. 17 (b), (c)). Then, similarly to Example 1, between $\epsilon_1 = 0.06$ and 0.07 bifurcation of Stokes curves occurs around the turning point near i (Figs. 16 and 17).

Now we give the connection matrices between $-\infty$ and $+\infty$ for $\epsilon_1 = 0.02$ and 0.07. If we assign α_j's and β_k's the Stokes coefficients as in Fig. 17 (a), the connection matrix M_2 for $\epsilon_1 = 0.02$ is

$$M_2 = \begin{pmatrix} 1 & 0 & \alpha_5 + \beta_2 \\ \alpha_3 & 1 & \alpha_4 \\ 0 & 0 & 1 \end{pmatrix} \begin{pmatrix} 1 & \alpha_2 & 0 \\ 0 & 1 & 0 \\ \alpha_0 + \beta_1 & \alpha_1 & 1 \end{pmatrix} \tag{64}$$

$$= \begin{pmatrix} 1 + (\alpha_0 + \beta_1)(\alpha_5 + \beta_2) & \alpha_2 + \alpha_1(\alpha_5 + \beta_2) & \alpha_5 + \beta_2 \\ \alpha_3 + \alpha_4(\alpha_0 + \beta_1) & 1 + \alpha_2\alpha_3 + \alpha_1\alpha_4 & \alpha_4 \\ \alpha_0 + \beta_1 & \alpha_1 & 1 \end{pmatrix}. \tag{65}$$

If we assign $\hat{\alpha}_j$'s and $\hat{\beta}_k$'s the Stokes coefficients as in Fig. 17 (d), the connection matrix $\hat{M}_2$ for $\epsilon_1 = 0.07$ is

$$\hat{M}_2 = \begin{pmatrix} 1 & 0 & \hat{\alpha}_5 + \hat{\beta}_2 \\ \hat{\alpha}_3 & 1 & \hat{\alpha}_4 + \hat{\alpha}_3\hat{\beta}_2 + \hat{\beta}_3 + \hat{\alpha}_3\hat{\alpha}_5 \\ 0 & 0 & 1 \end{pmatrix} \begin{pmatrix} 1 & \hat{\alpha}_2 & 0 \\ 0 & 1 & 0 \\ \hat{\alpha}_0 + \hat{\beta}_1 & \hat{\alpha}_1 + \hat{\alpha}_2\hat{\beta}_1 + \hat{\beta}_0 + \hat{\alpha}_0\hat{\alpha}_2 & 1 \end{pmatrix}. \tag{66}$$

Since $\hat{\beta}_0$ and $\hat{\beta}_3$ originate from the ordered crossing points A_0 and A_3 in Fig. 17 (b),

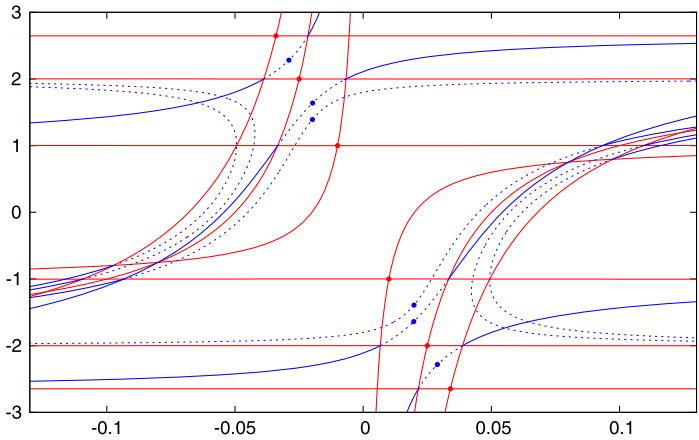

(a) $\epsilon_1 = 0.02$

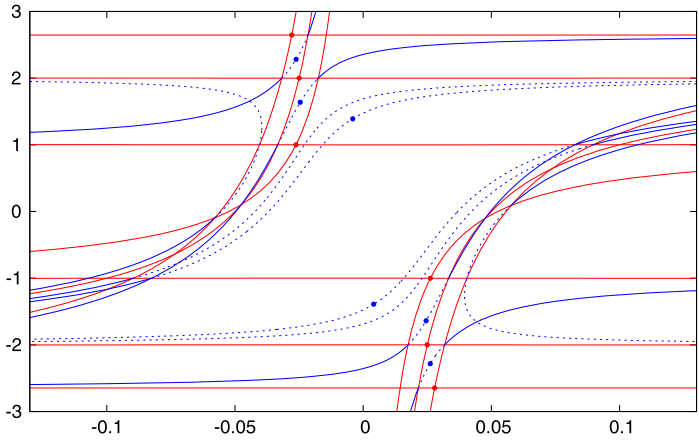

(b) $\epsilon_1 = 0.0525$

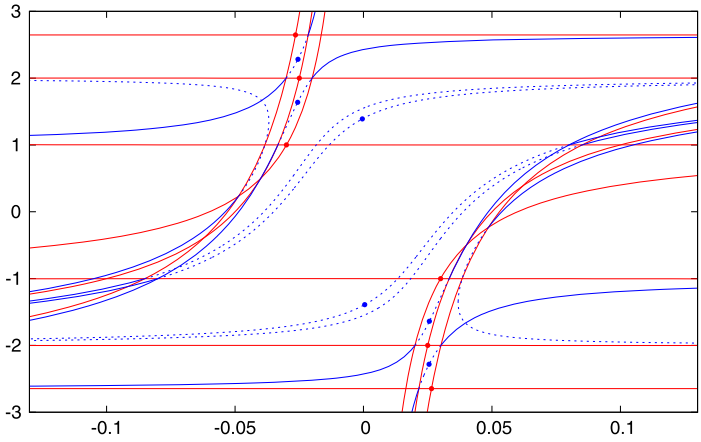

(c) $\epsilon_1 = 0.06$

Fig. 16. Change of Stokes geometry for Example 2 as $\epsilon_1 = 0.02 \to 0.07$ with $\epsilon_2 = 0.1$.

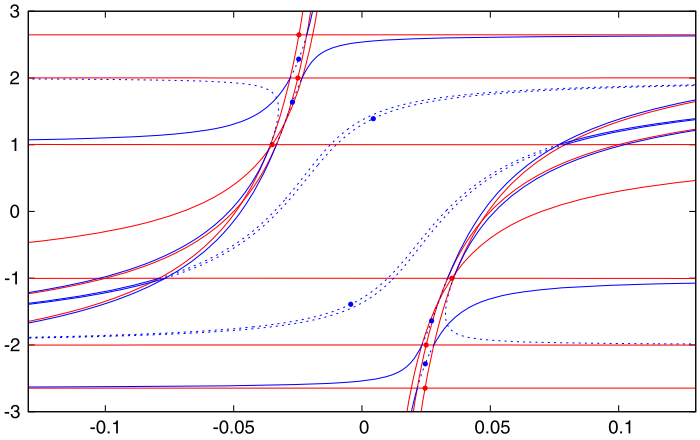

(d) $\epsilon_1 = 0.07$

Fig. 16. (*continued*)

$$\hat{\beta}_0 = -\hat{\alpha}_0\hat{\alpha}_2, \tag{67}$$

$$\hat{\beta}_3 = -\hat{\alpha}_3\hat{\alpha}_5 \tag{68}$$

hold, and $\hat{M}_2$ can be written as

$$\hat{M}_2 = \begin{pmatrix} 1 & 0 & \hat{\alpha}_5 + \hat{\beta}_2 \\ \hat{\alpha}_3 & 1 & \hat{\alpha}_4 + \hat{\alpha}_3\hat{\beta}_2 \\ 0 & 0 & 1 \end{pmatrix} \begin{pmatrix} 1 & \hat{\alpha}_2 & 0 \\ 0 & 1 & 0 \\ \hat{\alpha}_0 + \hat{\beta}_1 & \hat{\alpha}_1 + \hat{\alpha}_2\hat{\beta}_1 & 1 \end{pmatrix} \tag{69}$$

$$= \begin{pmatrix} 1 + (\hat{\alpha}_0 + \hat{\beta}_1)(\hat{\alpha}_5 + \hat{\beta}_2) & \hat{\alpha}_2 + (\hat{\alpha}_1 + \hat{\alpha}_2\hat{\beta}_1)(\hat{\alpha}_5 + \hat{\beta}_2) & \hat{\alpha}_5 + \hat{\beta}_2 \\ \hat{\alpha}_3 + (\hat{\alpha}_0 + \hat{\beta}_1)(\hat{\alpha}_4 + \hat{\alpha}_3\hat{\beta}_2) & 1 + \hat{\alpha}_2\hat{\alpha}_3 + (\hat{\alpha}_1 + \hat{\alpha}_2\hat{\beta}_1)(\hat{\alpha}_4 + \hat{\alpha}_3\hat{\beta}_2) & \hat{\alpha}_4 + \hat{\alpha}_3\hat{\beta}_2 \\ \hat{\alpha}_0 + \hat{\beta}_1 & \hat{\alpha}_1 + \hat{\alpha}_2\hat{\beta}_1 & 1 \end{pmatrix}. \tag{70}$$

Thus, again thanks to Theorem 1, we confirm that $M_2 = \hat{M}_2$.

Remark 4. Though we do not present here the connection matrices for $\epsilon_1 = 0.0525$ and 0.06, similarly to the case of Example 1, they equal M_2 and $\hat{M}_2$.

Now we compare the two terms in (1,3)-element of M_2. With $v(\simeq 0.0197 - 1.6379i)$ being the virtual turning point, the exponential factor of β_2 is

$$\exp\left[\frac{\eta}{i}\int_v^{t_0}(\rho_1 - \rho_3)\,dt\right]$$

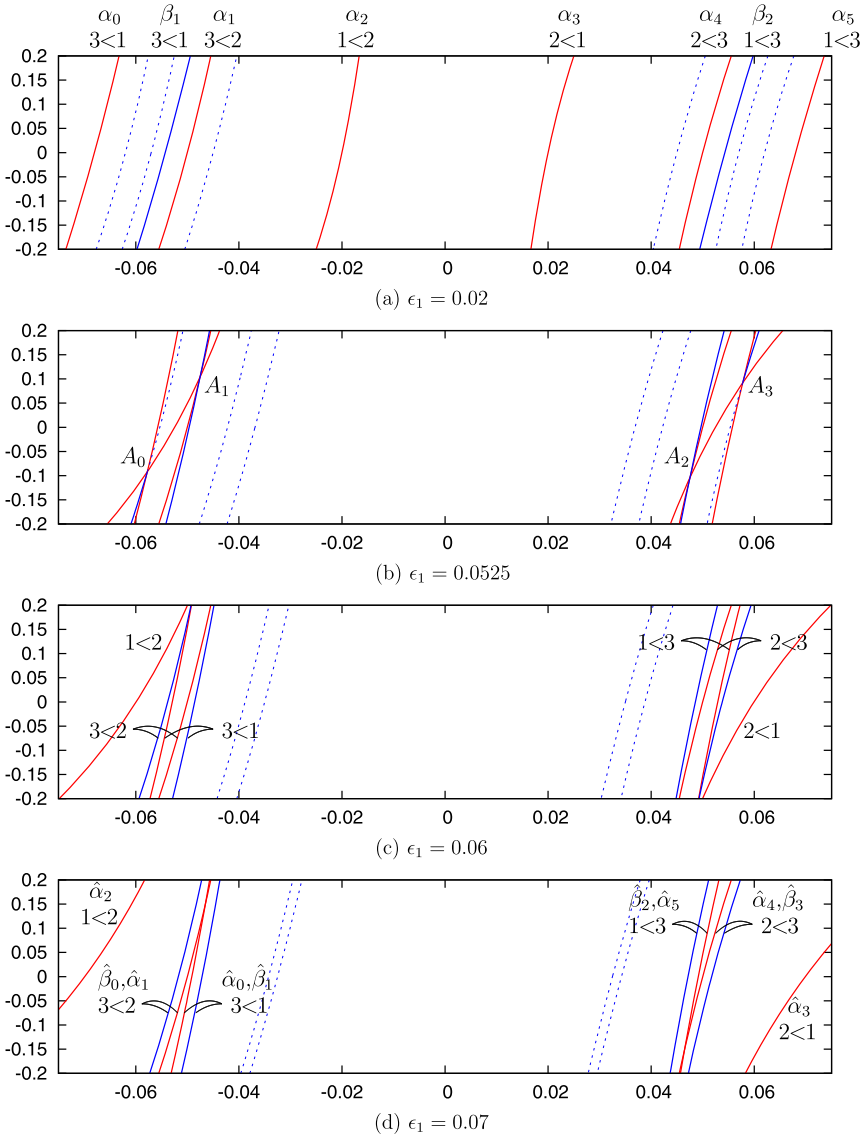

Fig. 17. Stokes curves near the real axis for Example 2 with $\epsilon_1 = 0.02, 0.0525, 0.6, 0.7$ and $\epsilon_2 = 0.1$.

$$= \exp\left[\frac{\eta}{i}\left\{\int_{-2i\sqrt{1+(i\epsilon_2/4)}}^{t_0}(\rho_2-\rho_3)\,dt + \int_{-i\sqrt{1+i\epsilon_1}}^{t_0}(\rho_1-\rho_2)\,dt\right\}\right], \tag{71}$$

and

$$\mathrm{Re}\left[\frac{\eta}{i}\int_{v}^{t_0}(\rho_1-\rho_3)\,dt\right] \simeq -10.0. \tag{72}$$

The exponential factor of α_5 is

$$\exp\left[\frac{\eta}{i}\int_{-\sqrt{7}i\sqrt{1+(i(2\epsilon_2-\epsilon_1)/7)}}^{t_0}(\rho_1-\rho_3)\,dt\right], \tag{73}$$

and

$$\mathrm{Re}\left[\frac{1}{i}\int_{-\sqrt{7}i\sqrt{1+(i(2\epsilon_2-\epsilon_1)/7)}}^{t_0}(\rho_1-\rho_3)\,dt\right]\simeq -12.3. \tag{74}$$

Therefore $|\beta_2|$ is much bigger than $|\alpha_5|$. Thus in transition $3\to 1$, the contribution by the virtual turning point v is much bigger than that by the ordinary turning point at $-\sqrt{7}i\sqrt{1+i(2\epsilon_2-\epsilon_1)/7}$.

4. Concluding remarks and future problems

In Example 1 with $\epsilon_1 = 0.02$ and $\epsilon_2 = 0.1$, though we compare $(1,3)$-element β_2 and (2,3)-element α_4 of the connection matrix M, β_2 itself has an important meaning; if we overlooked the contribution by virtual turning points, the element (or the corresponding transition probability) were exactly zero. However, there is an effect of virtual turning points and it is actually nonzero. Such effects of virtual turning points are already discussed in [14]. The consideration we have done in §3.1 of this paper reveals that a virtual turning point not only turns an element ($(1,3)$-element in this case) nonzero but also gives an effect which is greater than the contribution by an ordinary turning point in another element ($(2,3)$-element in this case). Therefore this example shows that the effect of virtual turning points is, even if it is exponentially small, non-negligible compared to the effect of ordinary turning points.

Meanwhile, in Example 2 with $\epsilon_1 = 0.02$ and $\epsilon_2 = 0.1$, we make comparison within a single matrix element. In the case of two-level systems, it is often the case that several ordinary turning points give contribution to an element and that the term with the biggest exponential factor gives a good approximation of the element. In the case of multi-level systems, at least theoretically we need to compare all the terms in an element, some of which are due to ordinary turning points and others are due to virtual turning points. The consideration in §3.2 shows that for a good approximation, we actually need to make comparison by taking account of virtual turning points; as a matter of fact, β_2 gives the main contribution to $(1,3)$-element of M_2. This indicates that virtual turning points are as important as (sometimes, more important than) ordinary turning points in non-adiabatic transition problems.

So far we have studied Examples 1 and 2 with values of perturbation parameters ϵ_1 and ϵ_2 so that we may avoid degeneration involving Stokes segments. Here a Stokes

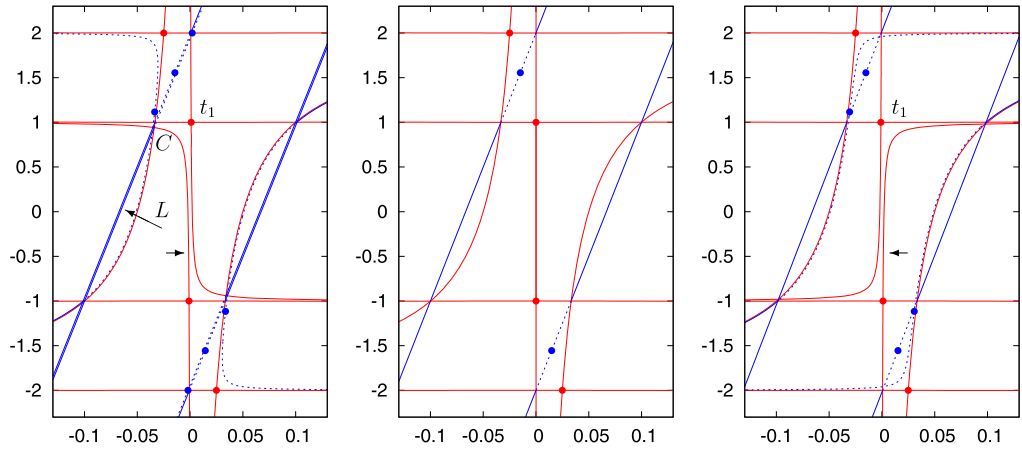

Fig. 18. Appearance of a Stokes segment in Example 1. In (b), two turning points at $\pm i$, both of which are of type $(1, 2)$, are connected by a Stokes curve.

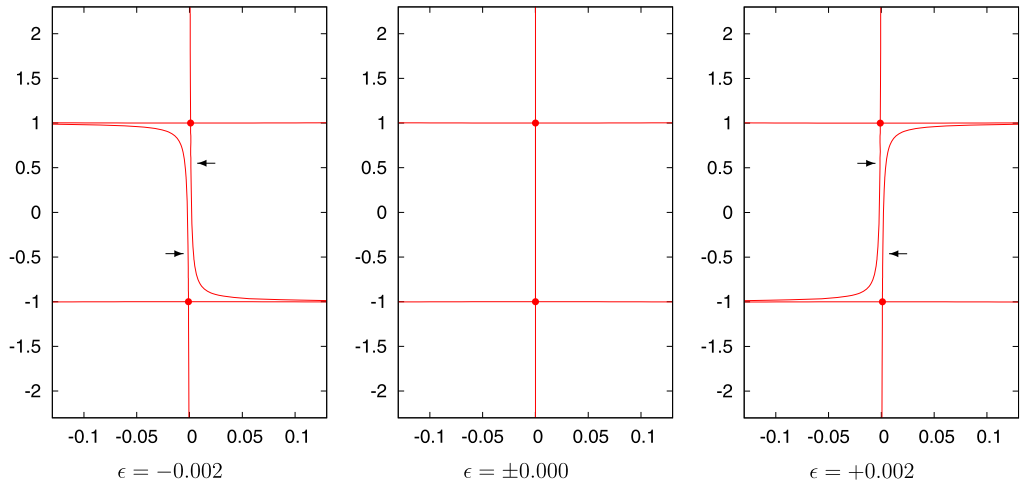

Fig. 19. Appearance of a Stokes segment in the two-level system given by $\rho_1 = t^2 + 1 + i\epsilon$, $\rho_2 = 0$.

segment is a Stokes curve which connects two turning points of the same type. Note that such degeneration actually occurs for some particular values of parameters. For example, if $\epsilon_1 = 0$ or $\epsilon_2 = 0$, Example 1 has a complex-conjugate pair of turning points of the same type. See Fig. 18. This kind of degeneration is observed also in two-level systems or second order single equations (Fig. 19), and it is closely related to the breakdown of Borel summability of WKB solutions ([18,7,17] etc.). As a parameter moves around a value where degeneration occurs, Borel sum of WKB solutions changes before and after the degeneration ("parametric Stokes phenomenon"), and therefore Stokes coefficients do as well. What is important there is that a couple of Stokes curves which coalesce into a Stokes segment changes its configuration discontinuously. See the Stokes curves

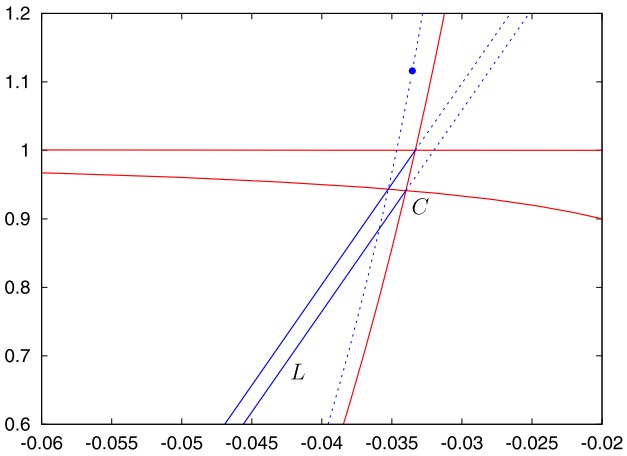

Fig. 20. Enlarged figure near the point C in Fig. 18 (a).

in Fig. 19 indicated by arrows. Now getting back to the three-level system, we look at Fig. 18 carefully. If we focus our attention only on the couple of Stokes curves, the variation of configuration is the same as that in the two-level system. Therefore we may expect that a parametric Stokes phenomenon occurs similarly for the three-level system. Meanwhile, such change of configuration of a couple of Stokes curves necessarily causes additional variation in the Stokes geometry, since this is a multi-level system. In fact, in Fig. 18 (a), the Stokes curve indicated by a horizontal arrow, which passes by the turning point t_1 seeing it on the right-hand side, crosses with a Stokes curve of different type at a point C, and causes another new Stokes curve L. (A neighborhood of the point C is enlarged in Fig. 20.) Now in Fig. 18 (c), which is obtained after the transition from Fig. 18 (a) via degeneration, the corresponding Stokes curve passes by the turning point t_1 seeing it on the left-hand side, and there is no new Stokes curve corresponding to L any more. Therefore there may be new kind of parametric Stokes phenomena peculiar to multi-level systems or higher order single equations. Studying this kind of new parametric Stokes phenomena would be important in the study of non-adiabatic transition problems.

In Example 2, we come across another phenomenon which is special to multi-level systems. Let ϵ_1 move from 0.07 to 0.08 with $\epsilon_2 = 0.1$ fixed (Fig. 21). Then between 0.078 and 0.08 we again encounter a discontinuous change of the geometry. We give enlarged pictures in Fig. 22 for ϵ_1 between 0.0784 and 0.0786. Between $\epsilon_1 = 0.078483$ and 0.078484 (Fig. 22), there seems to appear a triplet of Stokes segments, each of which connects an ordinary turning point and a virtual turning point. This phenomenon is already observed in the study of (higher order) Painlevé equations, in particular the so-called Noumi–Yamada systems, whose associated linear equations are of higher order ([12,13,8], cf. [10] also). There this kind of triplets are regarded as a natural generalization of the notion of Stokes segments, and geometric aspect of this phenomenon is studied by Honda [8,9]. However its analytic aspect such as explicit form of parametric Stokes phenomena is

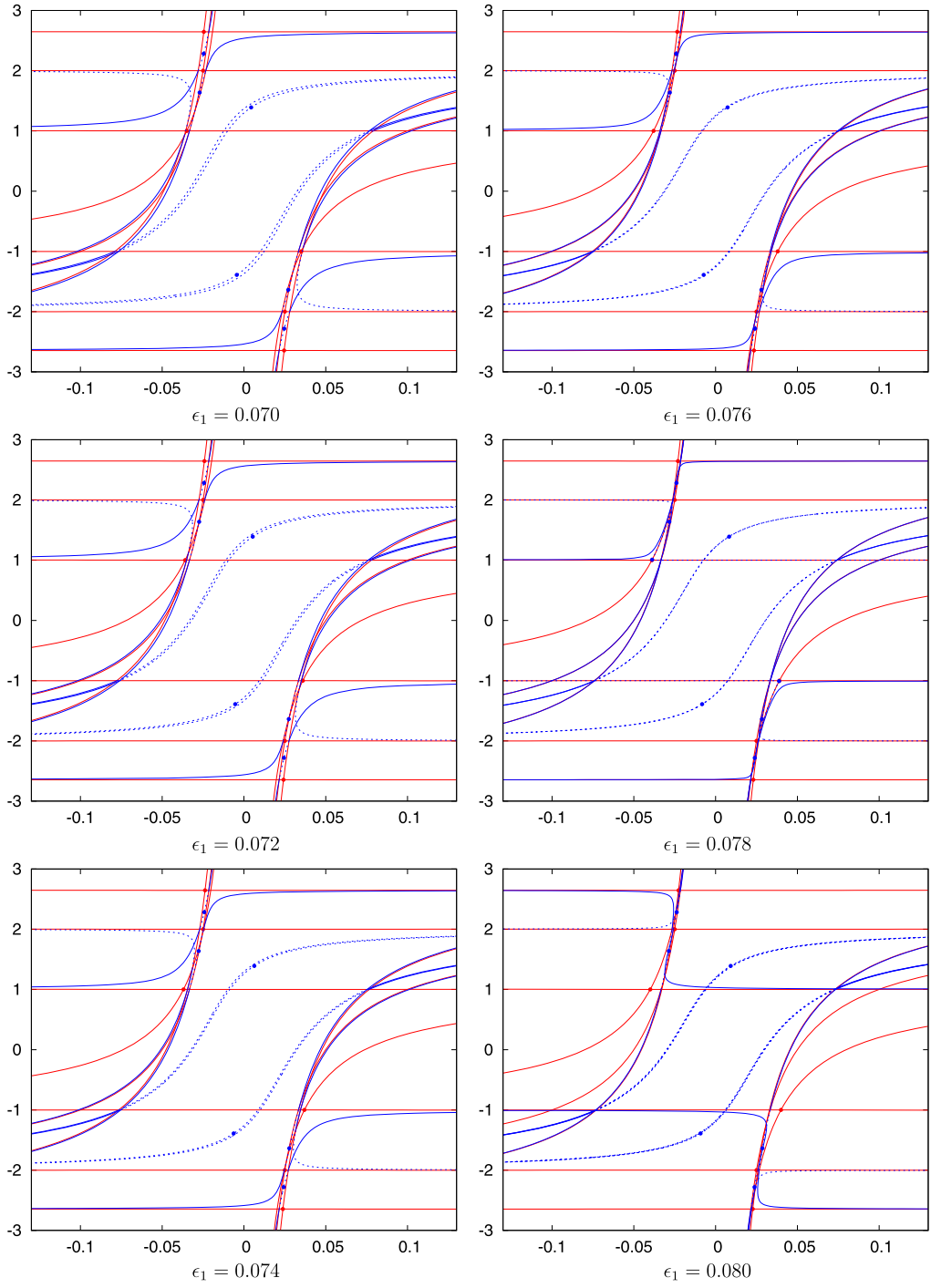

Fig. 21. Change of Stokes geometry for Example 2 as $\epsilon_1 = 0.07 \to 0.08$ with $\epsilon_2 = 0.1$. (Note that some ordinary Stokes curves overlap with new Stokes curves when $\epsilon_1 = 0.078$. In such situations overlapping Stokes curves are designated by blue.) (For interpretation of the references to color in this figure legend, the reader is referred to the web version of this article.)

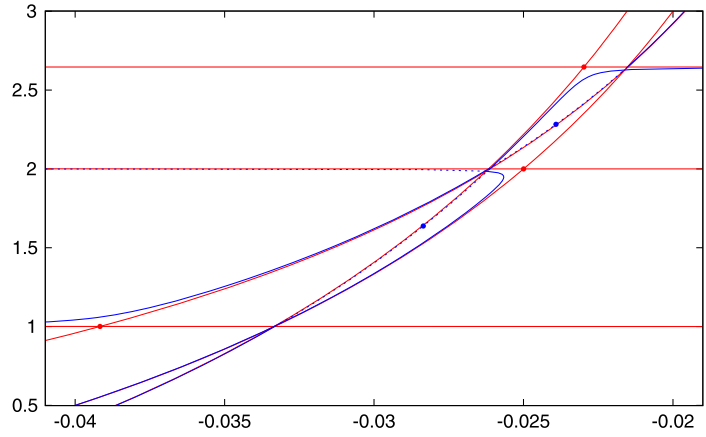

$\epsilon_1 = 0.0784$

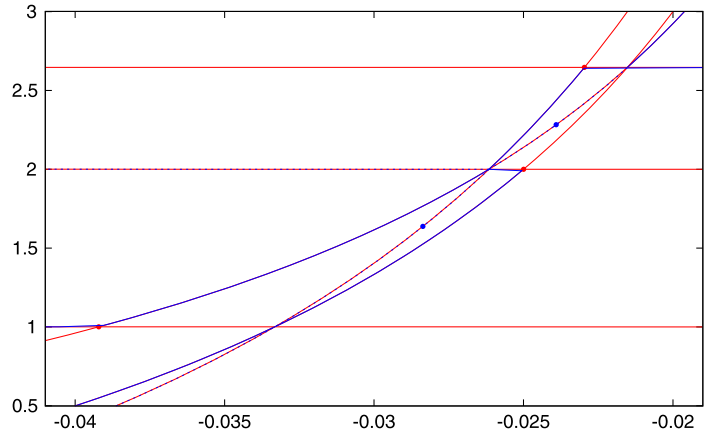

$\epsilon_1 = 0.078483$

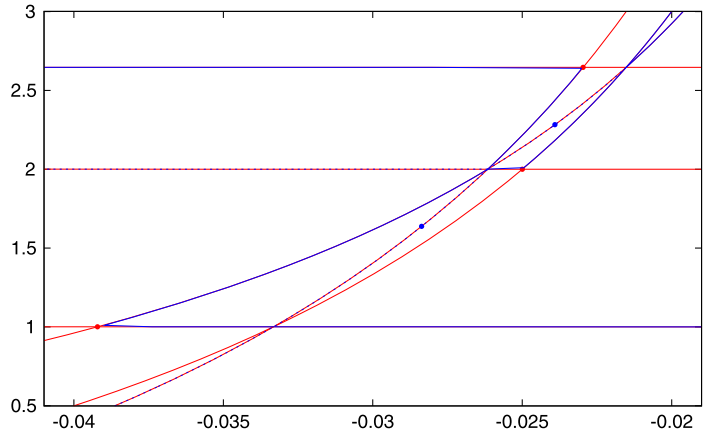

$\epsilon_1 = 0.078484$

Fig. 22. Change of Stokes geometry for Examples 2 as $\epsilon_1 = 0.0784 \to 0.0786$ with $\epsilon_2 = 0.1$. A part near $t = 2i$ is enlarged. (As in Fig. 21, overlapping Stokes curves are designated by blue for $\epsilon_1 = 0.078483$ and $\epsilon_1 = 0.078484$.) (For interpretation of the references to color in this figure legend, the reader is referred to the web version of this article.)

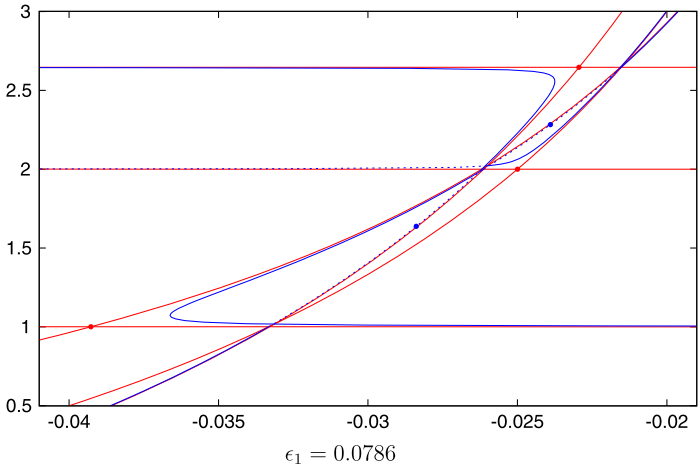

Fig. 22. (*continued*)

not investigated yet. A Stokes segment and a triplet of Stokes segments in non-adiabatic transition problems of three-level systems will be discussed in our forthcoming paper [15].

References

[1] T. Aoki, T. Kawai, S. Sasaki, A. Shudo, Y. Takei, Virtual turning points and bifurcation of Stokes curves for higher order ordinary differential equations, J. Phys. A: Math. Gen. 38 (15) (2005) 3317–3336.
[2] T. Aoki, T. Kawai, Y. Takei, New Turning Points in the Exact WKB Analysis for Higher-Order Ordinary Differential Equations, Analyse algébrique des perturbations singulières: Méthodes résurgentes, vol. 1, Hermann, 1994, pp. 69–84.
[3] T. Aoki, T. Kawai, Y. Takei, Exact WKB analysis of non-adiabatic transition probabilities for three levels, J. Phys. A: Math. Gen. 35 (10) (2002) 2401–2430.
[4] H. Berk, W.M. Nevins, K. Roberts, New Stokes' line in WKB theory, J. Math. Phys. 23 (6) (1982) 988–1002.
[5] S. Brundobler, V. Elser, *S*-matrix for generalized Landau–Zener problem, J. Phys. A: Math. Gen. 26 (5) (1993) 1211–1227.
[6] C. Carroll, F. Hioe, Transition probabilities for the three-level Landau–Zener model, J. Phys. A: Math. Gen. 19 (11) (1986) 2061–2073.
[7] E. Delabaere, H. Dillinger, F. Pham, Exact semiclassical expansions for one-dimensional quantum oscillators, J. Math. Phys. 38 (12) (1997) 6126–6184.
[8] N. Honda, Some examples of the Stokes geometry for Noumi–Yamada systems, RIMS Kôkyûroku 1516 (2006) 21–167 (in Japanese).
[9] N. Honda, On the Stokes geometry of the Noumi–Yamada system, RIMS Kôkyûroku Bessatsu B 2 (2007) 45–72.
[10] N. Honda, T. Kawai, Y. Takei, Virtual Turning Points, SpringerBriefs in Mathematical Physics, vol. 4, Springer, 2015.
[11] A. Joye, C.-E. Pfister, Complex WKB method for 3-level scattering systems, Asymptot. Anal. 23 (2) (2000) 91–109.
[12] S. Sasaki, On the role of virtual turning points in the deformation of higher order linear differential equations, RIMS Kôkyûroku 1433 (2005) 27–64.
[13] S. Sasaki, On the role of virtual turning points in the deformation of higher order linear differential equations, II, RIMS Kôkyûroku 1433 (2005) 65–109.
[14] Shinji Sasaki, On the inevitable influence of virtual turning points on the non-adiabatic transition probabilities for three-level systems, 2015, RIMS preprint, No. 1818.
[15] Shinji Sasaki, in preparation.

[16] A. Shudo, On the role of virtual turning points and new Stokes curves in multilevel non-adiabatic transition problems, RIMS Kôkyûroku 1516 (2006) 9–20 (in Japanese).
[17] Y. Takei, Sato's conjecture for the Weber equation and transformation theory for Schrödinger equations with a merging pair of turning points, RIMS Kôkyûroku Bessatsu B 10 (2008) 205–224.
[18] A. Voros, The return of the quartic oscillator—the complex WKB method, Ann. Inst. Henri Poincaré A, Phys. Théor. 39 (3) (1983) 211–338.